



Design, synthesis and biological evaluation of urea derivatives from *o*-hydroxybenzylamines and phenylisocyanate as potential FabH inhibitors

Zi-Lin Li, Qing-Shan Li, Hong-Jia Zhang, Yang Hu, Di-Di Zhu, Hai-Liang Zhu *

State Key Laboratory of Pharmaceutical Biotechnology, Nanjing University, Nanjing 210093, People's Republic of China

ARTICLE INFO

Article history:

Received 29 April 2011

Revised 16 June 2011

Accepted 16 June 2011

Available online 25 June 2011

Keywords:

FabH

Inhibitors

Antibacterial

o-Hydroxybenzylamines

Urea derivatives

ABSTRACT

FabH, β -ketoacyl-acyl carrier protein (ACP) synthase III, is a particularly attractive target, since it is central to the initiation of fatty acid biosynthesis and is highly conserved among Gram-positive and Gram-negative bacteria. A series of *o*-hydroxybenzylamines **1–16** and its corresponding new urea derivatives **17–32** were synthesized and fully characterized by spectroscopic methods and elemental analysis. This new urea derivatives class demonstrates strong antibacterial activity. *Escherichia coli* FabH inhibitory assay and docking simulation indicated that the compounds 1-(5-bromo-2-hydroxybenzyl)-1-(4-fluorophenyl)-3-phenylurea (**18**) and 1-(5-bromo-2-hydroxybenzyl)-1-(4-chlorophenyl)-3-phenylurea (**20**) were potent inhibitors of *E. coli* FabH.

Crown Copyright © 2011 Published by Elsevier Ltd. All rights reserved.

1. Introduction

The multi-drug resistance to most of all antibiotics has become a serious medical problem¹; therefore, there is an urgent need for development of new antibacterial agents with divergent and unique structure, which may act through novel target, surmounting the problem of acquired resistance.²

An attractive target is the fatty acid biosynthesis (FAB) in bacteria, which is an essential metabolic process and is required for cell viability and growth.³ The β -ketoacyl-acyl carrier protein synthase III (FabH) is one of functional enzymes in FAB, which initiates the FAB cycle by catalyzing the first condensation step between acetyl-CoA and malonyl-ACP (Fig. 1). The other bacterial condensing enzymes FabB and FabF, functioning later in the cycle, differ significantly from FabH in that they use acyl-ACP rather than acetyl-CoA as the primer for subsequent condensations and are hence nonredundant. As a result, no other known enzyme in the pathway appears to be able to accomplish this essential reaction, and thus, FabH appears to play a key role in the bacterial FAB cycle.⁴ Moreover, the key role and three-dimensional structure of the protein are highly conserved across various Gram-positive and Gram-negative bacteria and therefore its inhibitors can be potent antibiotics with broad-spectrum activity.⁵

o-Hydroxy diphenyl ethers is widely used as effective broad-spectrum antibiotic, which possess potent inhibiting effects on Gram-positive and Gram-negative bacteria, yeast and viruses.⁶ By

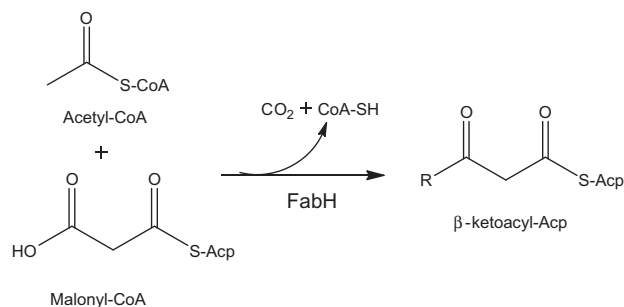


Figure 1. FabH-catalyzed initiation reaction of fatty acid biosynthesis.

simulating the natural substrate of specific bacteria enzyme, *o*-hydroxy diphenyl ethers can damage and block the normal biosynthesis of fatty acids.^{7–9} Its molecular fragment 'o-hydroxyphenyl' also shows favorable biological activity, which has a good affinity to coenzyme NAD⁺ and plays a key role in the process of inhibiting pathogens.^{10–12} Therefore, the 'o-hydroxyphenyl' fragment can be used as core structure unit to design antibacterial drugs.¹³

Phenylisocyanate is a widely used intermediate in organic synthesis,¹⁴ which can serve as the reactant to form urea derivatives. It has been well established that urea derivatives have got a significant place in modern medicinal chemistry. Urea derivatives have been reported in the literature as anticancer agent,¹⁵ anticonvulsant,¹⁶ and CXCR3 antagonist.¹⁷ Furthermore, in the past years, a large variety of urea derivatives were reported to function as inhibitors on HIV protease enzyme,¹⁸ receptor tyrosine kinases

* Corresponding author. Tel./fax: +86 25 83592672.

E-mail address: zhuhl@nju.edu.cn (H.-L. Zhu).

(RTKs),¹⁹ raf-1 kinases,²⁰ NADH oxidase,²¹ g-secretase,²² and acyl-coenzymeA-cholesterol acyltransferase (ACAT),²³ However, to our knowledge, few reports have been dedicated to the synthesis and FabH inhibitory activity of urea derivatives.

Herein, in continuation of our earlier studies on urea derivatives^{24,25} and an attempt to achieve potential antibacterial agents, we synthesized a series of *o*-hydroxybenzylamines and besides, through using these compounds as continuing point, designed and synthesized a new series of urea derivatives. The antimicrobial activity against two Gram-negative bacterial strains, *Escherichia coli* and *Pseudomonas fluorescense*, and two Gram-positive bacterial strains, *Bacillus subtilis* and *Staphylococcus aureus*, of these compounds were also been determined. Docking simulations were performed using the X-ray crystallographic structure of the FabH of *E. coli* complexed with the most potent inhibitors (**18** and **20**) to explore the binding modes of these compounds at the active site.

2. Results and discussion

2.1. Chemistry

A series of *o*-hydroxybenzylamines **1–16** and its corresponding urea derivatives **17–32** were synthesized by the route outlined in Scheme 1. The secondary amines (**1–16**) were obtained from the corresponding Schiff bases after the reduction reactions with sodium borohydride in 60–90% yield.²⁶ In the next step, the secondary amines were condensed with phenylisocyanate in chloroform as the solvent, affording the target compounds after 5 h for derivatives with electron-donating substituent groups (**17–22** and **25–30**), and after 10 h for the electron-withdrawing substituted derivatives (**23–24** and **31–32**). The reactions were monitored by thin layer chromatography (TLC) and the products were purified by recrystallization with ethanol and hexyl hydride or by column chromatography, with yields in the range of 50–80%. All of the synthetic

Table 1
Chemical structures of **1–32**

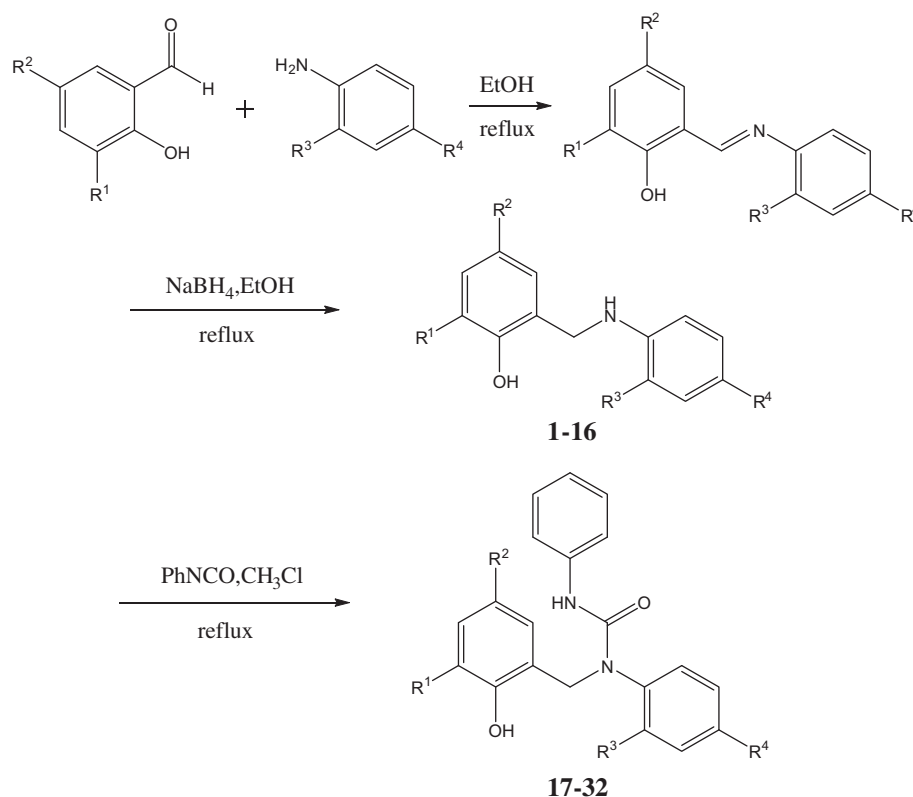
Compound	R ¹	R ²	R ³	R ⁴	Compound	R ¹	R ²	R ³	R ⁴
1	H	Br	F	H	17	H	Br	F	H
2	H	Br	H	F	18	H	Br	H	F
3	H	Br	Cl	H	19	H	Br	Cl	H
4	H	Br	H	Cl	20	H	Br	H	Cl
5	H	Br	Br	H	21	H	Br	Br	H
6	H	Br	H	Br	22	H	Br	H	Br
7	H	Br	H	CH ₃	23	H	Br	H	CH ₃
8	H	Br	H	OCH ₃	24	H	Br	H	OCH ₃
9	Br	Br	F	H	25	Br	Br	F	H
10	Br	Br	H	F	26	Br	Br	H	F
11	Br	Br	Cl	H	27	Br	Br	Cl	H
12	Br	Br	H	Cl	28	Br	Br	H	Cl
13	Br	Br	Br	H	29	Br	Br	Br	H
14	Br	Br	H	Br	30	Br	Br	H	Br
15	Br	Br	H	CH ₃	31	Br	Br	H	CH ₃
16	Br	Br	H	OCH ₃	32	Br	Br	H	OCH ₃

compounds gave satisfactory analytical and spectroscopic data, which in accordance with their depicted structures (Table 1).

2.2. Biological activity

2.2.1. Antibacterial activity

All the synthetic compounds (**1–32**) were evaluated for their antimicrobial activities against two Gram-negative bacterial strains: *E. coli* and *P. fluorescense* and two Gram-positive bacterial strains: *B. subtilis* and *S. aureus* by MTT method. The MICs (minimum inhibitory concentrations) of the compounds against these bacteria were presented in Table 2. Also included was the activity of standard antibacterial agent kanamycin B under identical conditions for comparison. The results revealed that most of the synthetic compounds exhibited significant antibacterial activities. Especially, the urea derivatives **17–32**, whose MICs values range



Scheme 1. The synthetic routes of compounds **1–32**.

Table 2
Antimicrobial activity of the synthesized compounds

Compound	Minimum inhibitory concentrations ($\mu\text{g/mL}$)			
	Gram-negative		Gram-positive	
	<i>E. coli</i>	<i>P. fluorescence</i>	<i>B. subtilis</i>	<i>S. aureus</i>
1	25	6.25	50	25
2	12.5	25	50	12.5
3	12.5	25	50	6.25
4	6.25	12.5	25	6.25
5	25	25	50	50
6	25	12.5	25	25
7	50	50	50	50
8	50	50	50	50
9	50	50	50	25
10	50	12.5	50	50
11	25	50	6.25	25
12	25	12.5	12.5	12.5
13	12.5	50	50	50
14	25	50	50	50
15	50	50	50	50
16	50	50	25	50
17	12.5	25	25	50
18	1.56	6.25	6.25	3.13
19	6.25	25	6.25	3.13
20	1.56	3.13	6.25	1.56
21	12.5	25	6.25	25
22	6.25	12.5	12.5	12.5
23	50	50	12.5	50
24	25	50	50	12.5
25	50	12.5	50	25
26	6.25	25	12.5	12.5
27	6.25	25	50	12.5
28	3.13	12.5	25	6.25
29	50	6.25	50	50
30	12.5	25	50	25
31	50	50	50	6.25
32	12.5	25	50	50
Kanamycin B	3.13	3.13	1.56	1.56

from 1.56 to 50 $\mu\text{g/mL}$, displayed higher antibacterial potencies than *o*-hydroxybenzylamines **1–16**, with MICs values ranging from 6.25 to 50 $\mu\text{g/mL}$, which showed the introduction of phenylisocyanate increased the hydrophobicity of *o*-hydroxybenzylamines and lead to the increase of the antibacterial activity.

Out of the 16 urea derivatives, compounds **18** and **20** displayed most potent activity with MIC values of both 1.56 $\mu\text{g/mL}$ against *E. coli* ATCC35218, which were superior to the positive control kanamycin B with corresponding MIC of 3.13 $\mu\text{g/mL}$. Compounds **28** showed significant activity with MIC values of 3.13 $\mu\text{g/mL}$ against *E. coli* ATCC35218, which was comparable to the positive control kanamycin B. Besides, the data showed compounds **18** and **20** exhibited favorable activity with MIC of 6.25, 6.25, 3.13 $\mu\text{g/mL}$ and 3.13, 6.25, 1.56 $\mu\text{g/mL}$ against *P. fluorescence*, *B. subtilis*, *S. aureus*, respectively, indicating that they possessing broad-spectrum antibacterial activity.

Based on the data obtained, we found that compounds with a bromine atom on the 5-position of salicylaldehyde displayed higher antibacterial activity against *E. coli* ATCC35218 than compounds with two bromine atoms on the 3-position and 5-position of salicylaldehyde. And the varieties of substituents of aniline such as halogen, methyl and methoxyl also lead to the different antibacterial activities of these urea derivatives. Among them, the derivatives which have electron-withdrawing substituents (such as F, Cl, Br) exhibited more potent activity against *E. coli* ATCC35218 than those have electron-donating substituents (such as CH_3 , OCH_3), and their MICs values range from 12.5 to 50 $\mu\text{g/mL}$. We proposed that electron-withdrawing halogen groups on aniline component were conducive to the antibacterial activity and compounds with CH_3 , OCH_3 substituents on aniline component were not favorable for activity.

Moreover, among derivatives with electron-withdrawing substituents, compounds **18**, **20**, **22**, **26**, **28** and **30** with *p*-substituted

F, Cl, Br group on aniline component showed significant antibacterial activity with MIC of 1.56–12.5 $\mu\text{g/mL}$ against *E. coli* ATCC35218. Compounds **17**, **19**, **21**, **25**, **27** and **29** with *o*-substituted electron-withdrawing group on aniline component exhibited less potent activity with MIC of 12.5–50 $\mu\text{g/mL}$. These results demonstrated that the synthetic urea derivatives with *p*-substituted halogen group on aniline component showed more potent antibacterial activity than those of *o*-substituted. Most significantly, the antibacterial activity of these compounds enhanced slightly in the order of substituent on aniline component: Br < F < Cl.

2.2.2. *E. coli* FabH inhibitory activity

The *E. coli* FabH inhibitory potency of the selected compounds **17–22** and **26–28** was examined and the results were summarized in Table 3. As shown in Table 3, among the tested compounds, compounds **18** and **20** showed potent inhibitory activity with IC_{50} of 6.6 and 4.7 μM , respectively, which were comparable to the positive control DDCP²⁷ with IC_{50} of 2.1 μM . Other tested compounds displayed moderate inhibitory activity with IC_{50} ranging from 10.1 to 71.7 μM . It suggested that the introduction of phenylisocyanate and the formation of urea structure were essential for the FabH inhibitory activity. It also can be seen from Table 3 that the selected compounds displayed low hemolytic activity.

2.3. Molecular docking study of synthetic compounds and binding model of compounds **18** and **20** and *E. coli* FabH

The binding affinity was evaluated by binding energy and inhibitory constant. Molecular docking of all the synthetic urea derivatives and *E. coli* FabH was performed on the binding model based

Table 3
E. coli FabH inhibitory activity of the selected compounds **17–22**, **26–28**

Compound	<i>E. coli</i> FabH IC_{50} (μM)	Hemolysis LC_{30} ^a (mg/mL)
17	37.4	>10
18	6.6	>10
19	21.8	>10
20	4.7	>10
21	56.4	>10
22	41.0	>10
26	71.7	>10
27	51.5	>10
28	10.1	>10
DDCP	2.1	>10

^a Lytic concentration 30%.

Table 4
Docking parameters of synthetic compounds

Compound	Binding energy ΔG_b (kcal/mol)	Inhibitory constant (fM)
17	−19.02	38.36
18	−21.88	1.61
19	−18.97	12.42
20	−21.08	1.03
21	−19.61	7.06
22	−19.46	5.48
23	−19.31	57.82
24	−18.97	35.61
25	−19.22	8.1
26	−19.3	7.13
27	−19.2	8.43
28	−20.02	9.11
29	−16.53	759.09
30	−18.78	17.23
31	−18.57	24.59
32	−17.35	191.97

on the *E. coli* FabH-CoA complex structure (1HNJ.pdb).²⁸ The FabH active site generally contains a catalytic triad tunnel consisting of Cys-His-Asn, which is conserved in various bacteria. This catalytic triad plays an important role in the regulation of chain elongation and substrate binding. Since the alkyl chain of CoA is broken by Cys of the catalytic triad of FabH, interactions between Cys and substrate appear to play an important role in substrate binding (Fig. 1). Qiu et al. have refined three-dimensional structure of *E. coli* FabH in the presence and absence of malonyl-CoA by X-ray

spectroscopy. Since, malonyl moiety is degraded by *E. coli* FabH, molecular docking studies for FabH and malonyl-CoA was carried out to identify a plausible malonyl-binding mode.²⁸ They found that in one of the binding modes appeared in the lower scored conformations, the malonyl carboxylate formed hydrogen bonds to the backbone nitrogen of Phe304. Enlightened by this report, Kim and co-workers designed pharmacophoremaps considering the interaction with Phe304 and performed receptor-oriented pharmacophore based in silico screening of *E. coli* FabH.³ YKAs3003, a

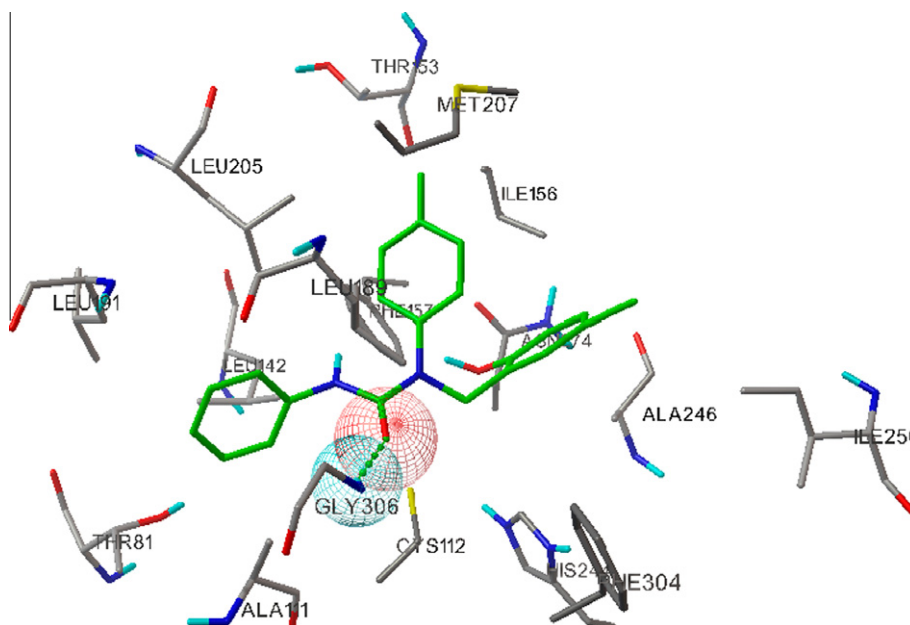


Figure 2. Binding model of compound **18** and *E. coli* FabH. H-bonds are displayed as dashed lines. Amino hydrogen of Gly306 forms hydrogen bond with oxygen atom of urea structure of compound **18**.

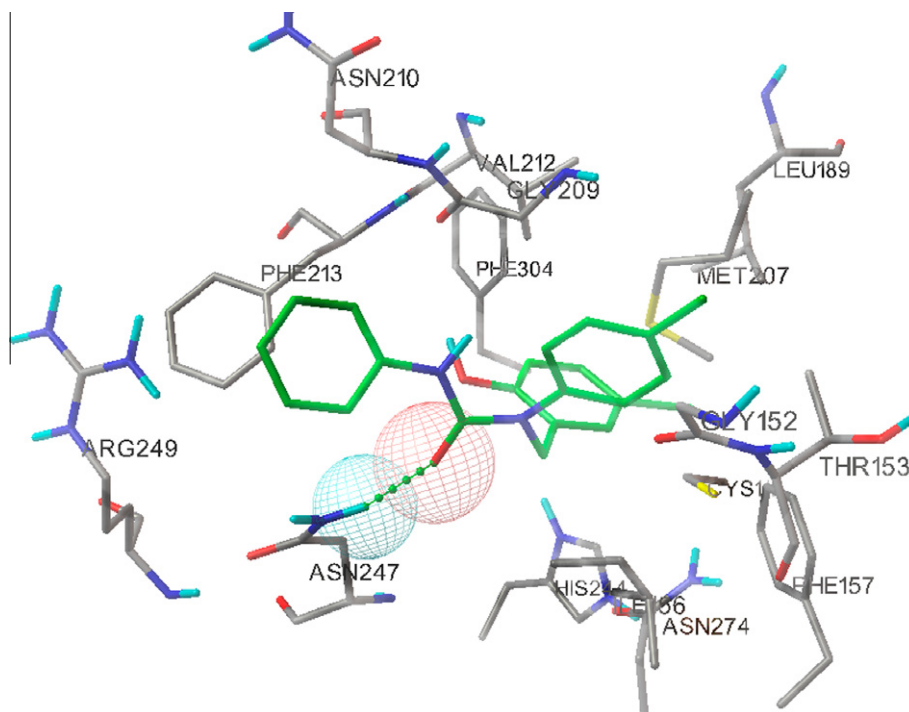


Figure 3. Binding model of compound **20** and *E. coli* FabH. H-bonds are displayed as dashed lines. Amino hydrogen of Asn247 forms hydrogen bond with oxygen atom of urea structure of compound **20**.

Schiff base condensed by 4-hydroxy salicylaldehyde and cyclohexanamine, was hit by pharmacophore map I consisting of three features (two hydrogen bond donors that involving the backbone oxygen of Phe304 and Gly209, respectively, and one hydrophobic interaction with Ile156, Phe157 and Met207).

The binding affinity of the synthetic urea derivatives and *E. coli* FabH is depicted in Table 4. As shown in Table 4, the results of binding energy and inhibitory constant almost have the same trend with the structure–activity relationships. Structure–activity relationships in compounds **17–32** demonstrated that compounds with different substituent group exhibit different bioactivity. Among them, compounds **18** and **20** showed minimum antibacterial data. Besides, in parameter of binding affinity, compounds **18** and **20** also exhibit favorable data, with free binding energy of -21.88 and -21.08 kcal/mol, inhibitory constant of 1.61 and 1.03 fM, respectively. The estimated free binding energy of other compounds (**17**, **19**, **21–32**) are ranging from -20.02 to -16.53 kcal/mol and inhibitory constants are ranging from 5.48 to 759.09 fM, respectively. This molecular docking result is along with the biological assay data, suggesting that compounds **18** and **20** are potential inhibitors of *E. coli* FabH.

Based on these facts, compounds **18** and **20** with the most potent inhibitory activity were selected for further molecular docking study. The binding models of compounds **18**, **20** and *E. coli* FabH are depicted in Figures 2 and 3, respectively. In the binding model of compound **18** and *E. coli* FabH, amino hydrogen of Gly306 forms hydrogen bond (H–O...H: 2.10 Å, 142.57°) with oxygen atom of urea structure of compound **18**. The urea structure of compound **18** projects into a hydrophobic interaction region of FabH, which contained the side chains: Leu142, Leu189, Asn274 and Phe157. Amino hydrogen of Asn247 also forms hydrogen bond (H–O...H: 1.91 Å, 159.87°) with oxygen atom of urea structure of compound **20** and it exits a hydrophobic interaction region, comprised of Phe213, Phe304, Met207 and Gly152. The hydrophobic interactions between **18**, **20** and FabH were important for their potent inhibitory activity.

3. Conclusions

In summary, a series of *o*-hydroxybenzylamines **1–16** and its corresponding new urea derivatives **17–32** were prepared and tested for their inhibitory activity against *E. coli*, *P. fluorescens*, *B. subtilis*, and *S. aureus*. Many synthetic compounds showed potent antibacterial and *E. coli* FabH inhibitory activities with compounds **18** and **20** being the most potent compounds. Preliminary structure–activity relationships and molecular modeling study provided further insight into interactions between the enzyme and its ligand. The results provided valuable information for the design of *E. coli* FabH inhibitors as antibiotics.

4. Experimental section

4.1. Chemistry

All chemicals (reagent grade) used were purchased from Sigma Aldrich (USA) and Sinopharm Chemical Reagent Co., Ltd (China). Melting points (uncorrected) were determined on a XT4 MP apparatus (Taike Corp., Beijing, China). ESI-MS spectra were recorded on a Mariner System 5304 Mass spectrometer., and ¹H NMR spectra were recorded on a Bruker DPX 300 model Spectrometer at 25 °C with TMS and solvent signals allotted as internal standards. Chemical shifts were reported in ppm (δ). Elemental analyses were performed on a CHN-O-Rapid instrument and were within $\pm 0.4\%$ of the theoretical values. TLC was run on the silica gel coated aluminum sheets (Silica Gel 60 Å GF₂₅₄, E. Merk, Germany) and visualized in UV light (254 nm).

4.2. General method for synthesis of *o*-hydroxybenzylamines **1–16** and corresponding urea derivatives **17–32**

Anilines (4.0 mmol) in ethanol (10 mL) was treated with equimolar quantities of substituted salicylaldehydes. The mixture was refluxed for 4–6 h, and the reaction was monitored by TLC. The products thus precipitated were filtered and recrystallized in ethanol. Without further purification, to an ethanolic solution of synthesized Schiff bases, NaBH₄ (4.0 mmol) was dissolved in ethanol and slowly added in an ice bath with stirring. The mixture was refluxed for 2–3 h. After that, the solvent was evaporated and water (15 mL) was added. The product extraction was carried out with CH₂Cl₂ (3 × 20 mL). The organic layer was dried over anhydrous Na₂SO₄ and concentrated. The residue was purified by recrystallization from ethanol to afford white or yellow crystals (**1–16**).

To chloroform solution of secondary amines (**1–16**), phenylisocyanate (1:1) was slowly added with stirring. The mixture was refluxed 5–10 h. The completion of reaction was checked by TLC. The CHCl₃ was removed under reduced pressure and the crude product was purified by recrystallization with ethanol and hexyl hydride or by column chromatography to afford urea derivatives (**17–32**).

4.2.1. 4-Bromo-2-((2-fluorophenyl)amino)methylphenol (**1**)

White crystal, yield 69%, mp: 101–102 °C, ¹H NMR (300 MHz, CDCl₃): 4.42 (s, 2H); 6.12 (s, 1H); 6.79 (d, *J* = 8.4 Hz, 1H); 6.84–6.94 (m, 2H); 6.79 (d, *J* = 7.5 Hz, 2H); 7.35 (d, *J* = 2.6 Hz, 2H); 8.13 (s, 1H). ESI-MS C₁₃H₁₁BrFNO [M+H]⁺ 296.0. Anal. Calcd for C₁₃H₁₁BrFNO: C, 52.73; H, 3.74; N, 4.73. Found: C, 52.69; H, 3.72; N, 4.72.

4.2.2. 4-Bromo-2-((4-fluorophenyl)amino)methylphenol (**2**)

White crystal, yield 82%, mp: 107–108 °C, ¹H NMR (300 MHz, CDCl₃): 4.36 (s, 2H); 6.13 (s, 1H); 6.76–6.80 (m, 3H); 6.95 (t, *J* = 5.2 Hz, 2H); 7.29 (d, *J* = 1.5 Hz, 1H); 7.31 (d, *J* = 1.5 Hz, 1H); 8.45 (s, 1H). ESI-MS C₁₃H₁₁BrFNO [M+H]⁺ 296.0. Anal. Calcd for C₁₃H₁₁BrFNO: C, 52.73; H, 3.74; N, 4.73. Found: C, 52.70; H, 3.71; N, 4.75.

4.2.3. 4-Bromo-2-((2-chlorophenyl)amino)methylphenol (**3**)

White crystal, yield 70%, mp: 112–113 °C, ¹H NMR (300 MHz, CDCl₃): 4.37 (s, 2H); 6.12 (s, 1H); 6.73–6.78 (m, 3H); 7.01–7.04 (m, 2H); 7.27 (d, *J* = 1.5 Hz, 1H); 7.29 (d, *J* = 1.5 Hz, 1H); 8.17 (s, 1H). ESI-MS C₁₃H₁₁BrClNO [M+H]⁺ 312.0. Anal. Calcd for C₁₃H₁₁BrClNO: C, 49.95; H, 3.55; N, 4.48. Found: C, 49.81; H, 3.56; N, 4.47.

4.2.4. 4-Bromo-2-((4-chlorophenyl)amino)methylphenol (**4**)

White crystal, yield 78%, mp: 109–110 °C, ¹H NMR (300 MHz, CDCl₃): 4.36 (s, 2H); 6.11 (s, 1H); 6.74–6.77 (m, 3H); 7.18–7.21 (m, 2H); 7.27 (d, *J* = 1.5 Hz, 1H); 7.31 (dd, *J* = 5.1, 1.5 Hz, 1H); 8.23 (s, 1H). ESI-MS C₁₃H₁₁BrClNO [M+H]⁺ 312.0. Anal. Calcd for C₁₃H₁₁BrClNO: C, 49.95; H, 3.55; N, 4.48. Found: C, 49.86; H, 3.57; N, 4.46.

4.2.5. 4-Bromo-2-((2-bromophenyl)amino)methylphenol (**5**)

Yellow crystal, yield 83%, mp: 123–124 °C, ¹H NMR (300 MHz, CDCl₃): 4.36 (s, 2H); 6.12 (s, 1H); 6.76–6.79 (m, 3H); 7.20–7.24 (m, 3H); 7.32 (d, *J* = 1.5 Hz, 1H); 8.32 (s, 1H). ESI-MS C₁₃H₁₁Br₂NO [M+H]⁺ 355.9. Anal. Calcd for C₁₃H₁₁Br₂NO: C, 43.73; H, 3.11; N, 3.92. Found: C, 43.87; H, 3.08; N, 3.91.

4.2.6. 4-Bromo-2-((4-bromophenyl)amino)methylphenol (**6**)

Yellow crystal, yield 81%, mp: 117–118 °C, ¹H NMR (300 MHz, CDCl₃): 4.37 (s, 2H); 6.10 (s, 1H); 6.71 (dd, *J* = 6.8, 2.0 Hz, 2H); 6.76–6.79 (m, 1H); 7.30–7.37 (m, 4H); 8.32 (s, 1H). ESI-MS

$C_{13}H_{11}Br_2NO$ $[M+H]^+$ 355.9. Anal. Calcd for $C_{13}H_{11}Br_2NO$: C, 43.73; H, 3.11; N, 3.92. Found: C, 43.79; H, 3.11; N, 3.93.

4.2.7. 4-Bromo-2-((*p*-tolylamino)methyl)phenol (7)

White crystal, yield 90%, mp: 97–98 °C, 1H NMR (300 MHz, $CDCl_3$): 2.27 (s, 3H); 4.36 (s, 2H); 6.12 (s, 1H); 6.74–6.76 (m, 3H); 7.05 (dd, $J = 5.1, 0.4$ Hz, 2H); 7.25 (d, $J = 2.0$ Hz, 1H); 7.05 (dd, $J = 5.2, 1.5$ Hz, 1H); 8.13 (s, 1H). ESI-MS $C_{14}H_{14}BrNO$ $[M+H]^+$ 292.0. Anal. Calcd for $C_{14}H_{14}BrNO$: C, 57.55; H, 4.83; N, 4.79. Found: C, 57.63; H, 4.80; N, 4.77.

4.2.8. 4-Bromo-2-(((4-methoxyphenyl)amino)methyl)phenol (8)

Lavender crystal, yield 65%, mp: 105–106 °C, 1H NMR (300 MHz, $CDCl_3$): 3.78 (s, 3H); 4.37 (s, 2H); 6.11 (s, 1H); 6.76–6.79 (m, 1H); 6.83 (m, 4H); 7.25 (d, $J = 2.4$ Hz, 1H); 7.29–7.33 (m, 1H); 8.16 (s, 1H). ESI-MS $C_{14}H_{14}BrNO_2$ $[M+H]^+$ 308.0. Anal. Calcd for $C_{14}H_{14}BrNO_2$: C, 54.56; H, 4.58; N, 4.55. Found: C, 54.47; H, 4.60; N, 4.57.

4.2.9. 2,4-Dibromo-6-(((2-fluorophenyl)amino)methyl)phenol (9)

Yellow crystal, yield 76%, mp: 114–115 °C, 1H NMR (300 MHz, $CDCl_3$): 4.42 (s, 2H); 6.17 (s, 1H); 6.70–6.80 (m, 2H); 6.97–7.05 (m, 2H); 7.32 (d, $J = 2.4$ Hz, 1H); 7.56 (d, $J = 2.4$ Hz, 1H); 8.20 (s, 1H). ESI-MS $C_{13}H_{10}Br_2FNO$ $[M+H]^+$ 374.0. Anal. Calcd for $C_{13}H_{10}Br_2FNO$: C, 41.63; H, 2.69; N, 3.73. Found: C, 41.67; H, 2.70; N, 3.76.

4.2.10. 2,4-Dibromo-6-(((4-fluorophenyl)amino)methyl)phenol (10)

Yellow crystal, yield 79%, mp: 125–126 °C, 1H NMR (300 MHz, $CDCl_3$): 4.24 (s, 2H); 6.12 (s, 1H); 6.53 (dd, $J = 8.9, 4.5$ Hz, 2H); 6.91 (t, $J = 8.9$ Hz, 2H); 7.32 (d, $J = 2.0$ Hz, 1H); 7.59 (d, $J = 2.2$ Hz, 1H); 9.63 (s, 1H). ESI-MS $C_{13}H_{10}Br_2FNO$ $[M+H]^+$ 374.0. Anal. Calcd for $C_{13}H_{10}Br_2FNO$: C, 41.63; H, 2.69; N, 3.73. Found: C, 41.52; H, 2.70; N, 3.73.

4.2.11. 2,4-Dibromo-6-(((2-chlorophenyl)amino)methyl)phenol (11)

White crystal, yield 83%, mp: 124–125 °C, 1H NMR (300 MHz, $CDCl_3$): 4.45 (s, 2H); 5.78 (s, 1H); 6.67 (dd, $J = 8.0, 1.3$ Hz, 1H); 6.71–6.77 (m, 1H); 7.10–7.16 (m, 1H); 7.28–7.33 (m, 2H); 7.56 (d, $J = 2.4$ Hz, 1H); 9.61 (s, 1H). ESI-MS $C_{13}H_{10}Br_2ClNO$ $[M+H]^+$ 389.9. Anal. Calcd for $C_{13}H_{10}Br_2ClNO$: C, 39.88; H, 2.57; N, 3.58. Found: C, 43.00; H, 2.56; N, 3.59.

4.2.12. 2,4-Dibromo-6-(((4-chlorophenyl)amino)methyl)phenol (12)

White crystal, yield 87%, mp: 130–131 °C, 1H NMR (300 MHz, $CDCl_3$): 4.23 (s, 2H); 6.36 (s, 1H); 6.51–6.54 (m, 2H); 7.07 (dd, $J = 6.8, 2.0$ Hz, 2H); 7.27 (d, $J = 2.4$ Hz, 1H); 7.58 (d, $J = 2.4$ Hz, 1H); 9.59 (s, 1H). ESI-MS $C_{13}H_{10}Br_2ClNO$ $[M+H]^+$ 389.9. Anal. Calcd for $C_{13}H_{10}Br_2ClNO$: C, 39.88; H, 2.57; N, 3.58. Found: C, 39.79; H, 2.55; N, 3.57.

4.2.13. 2,4-Dibromo-6-(((2-bromophenyl)amino)methyl)phenol (13)

Yellow crystal, yield 85%, mp: 128–129 °C, 1H NMR (300 MHz, $CDCl_3$): 4.46 (s, 2H); 5.80 (s, 1H); 6.66–6.72 (m, 2H); 6.92 (s, 1H); 7.15–7.21 (m, 1H); 7.47–7.50 (m, 1H); 7.57 (d, $J = 2.4$ Hz, 1H); 9.56 (s, 1H). ESI-MS $C_{13}H_{10}Br_3NO$ $[M+H]^+$ 433.8. Anal. Calcd for $C_{13}H_{10}Br_3NO$: C, 35.82; H, 2.31; N, 3.21. Found: C, 35.64; H, 2.33; N, 3.22.

4.2.14. 2,4-Dibromo-6-(((4-bromophenyl)amino)methyl)phenol (14)

Yellow crystal, yield 89%, mp: 126–127 °C, 1H NMR (300 MHz, $CDCl_3$): 4.36 (s, 2H); 6.08 (s, 1H); 6.59 (dd, $J = 6.8, 2.2$ Hz, 2H);

7.28–7.31 (m, 3H); 7.56 (d, $J = 2.2$ Hz, 1H); 9.55 (s, 1H). ESI-MS $C_{13}H_{10}Br_3NO$ $[M+H]^+$ 433.8. Anal. Calcd for $C_{13}H_{10}Br_3NO$: C, 35.82; H, 2.31; N, 3.21. Found: C, 35.98; H, 2.34; N, 3.20.

4.2.15. 2,4-Dibromo-6-((*p*-tolylamino)methyl)phenol (15)

White crystal, yield 80%, mp: 123–124 °C, 1H NMR (300 MHz, $CDCl_3$): 2.27 (s, 3H); 4.40 (s, 2H); 6.12 (s, 1H); 6.72 (d, $J = 8.4$ Hz, 2H); 7.06 (d, $J = 8.2$ Hz, 2H); 7.25 (d, $J = 3.8$ Hz, 1H); 7.58 (d, $J = 2.4$ Hz, 1H); 9.56 (s, 1H). ESI-MS $C_{14}H_{13}Br_2NO$ $[M+H]^+$ 369.9. Anal. Calcd for $C_{14}H_{13}Br_2NO$: C, 45.32; H, 3.53; N, 3.77. Found: C, 45.36; H, 3.56; N, 3.76.

4.2.16. 2,4-Dibromo-6-(((4-methoxyphenyl)amino)methyl)phenol (16)

Lavender crystal, yield 78%, mp: 119–120 °C, 1H NMR (300 MHz, $CDCl_3$): 3.76 (s, 3H); 4.36 (s, 2H); 6.10 (s, 1H); 6.75–6.83 (m, 4H); 7.23 (d, $J = 2.4$ Hz, 1H); 7.57 (d, $J = 2.4$ Hz, 1H); 9.56 (s, 1H). ESI-MS $C_{14}H_{13}Br_2NO_2$ $[M+H]^+$ 385.9. Anal. Calcd for $C_{14}H_{13}Br_2NO_2$: C, 43.44; H, 3.39; N, 3.62. Found: C, 43.51; H, 3.36; N, 3.61.

4.2.17. 1-(5-Bromo-2-hydroxybenzyl)-1-(2-fluorophenyl)-3-phenylurea (17)

White powder, yield 56%, mp: 140–141 °C, 1H NMR (300 MHz, $CDCl_3$): 4.68 (s, 2H); 6.11 (s, 1H); 6.69 (d, $J = 1.5$ Hz, 1H); 7.10–7.12 (m, 1H); 7.17–7.20 (m, 2H); 7.24–7.30 (m, 4H); 7.47–7.53 (m, 3H); 7.60 (d, $J = 1.5$ Hz, 1H); 10.68 (s, 1H). ESI-MS $C_{20}H_{16}BrFN_2O_2$ $[M+H]^+$ 415.0. Anal. Calcd for $C_{20}H_{16}BrFN_2O_2$: C, 57.85; H, 3.88; N, 6.75. Found: C, 57.99; H, 3.87; N, 6.76.

4.2.18. 1-(5-Bromo-2-hydroxybenzyl)-1-(4-fluorophenyl)-3-phenylurea (18)

White powder, yield 62%, mp: 139–140 °C, 1H NMR (300 MHz, $CDCl_3$): 4.64 (s, 2H); 6.10 (s, 1H); 6.70 (d, $J = 2.4$ Hz, 1H); 7.04–7.06 (m, 1H); 7.21–7.24 (m, 2H); 7.27–7.29 (m, 4H); 7.49–7.52 (m, 3H); 7.61 (d, $J = 1.5$ Hz, 1H); 10.73 (s, 1H). ESI-MS $C_{20}H_{16}BrFN_2O_2$ $[M+H]^+$ 415.0. Anal. Calcd for $C_{20}H_{16}BrFN_2O_2$: C, 57.85; H, 3.88; N, 6.75. Found: C, 57.81; H, 3.90; N, 6.77.

4.2.19. 1-(5-Bromo-2-hydroxybenzyl)-1-(2-chlorophenyl)-3-phenylurea (19)

White powder, yield 71%, mp: 147–148 °C, 1H NMR (300 MHz, $CDCl_3$): 4.68 (s, 2H); 6.07 (s, 1H); 6.71 (d, $J = 1.4$ Hz, 1H); 7.05–7.08 (m, 1H); 7.13–7.15 (m, 3H); 7.22–7.24 (m, 4H); 7.41–7.44 (m, 2H); 7.62 (d, $J = 1.5$ Hz, 1H); 10.65 (s, 1H). ESI-MS $C_{20}H_{16}BrClN_2O_2$ $[M+H]^+$ 431.0. Anal. Calcd for $C_{20}H_{16}BrClN_2O_2$: C, 55.64; H, 3.74; N, 6.49. Found: C, 55.69; H, 3.76; N, 6.48.

4.2.20. 1-(5-Bromo-2-hydroxybenzyl)-1-(4-chlorophenyl)-3-phenylurea (20)

White powder, yield 72%, mp: 157–158 °C, 1H NMR (300 MHz, $CDCl_3$): 4.71 (s, 2H); 6.06 (s, 1H); 6.72 (d, $J = 2.6$ Hz, 1H); 6.86 (d, $J = 8.6$ Hz, 1H); 7.02–7.07 (m, 1H); 7.11–7.15 (m, 2H); 7.22–7.25 (m, 5H); 7.46–7.51 (m, 2H); 9.92 (s, 1H). ESI-MS $C_{20}H_{16}BrClN_2O_2$ $[M+H]^+$ 431.0. Anal. Calcd for $C_{20}H_{16}BrClN_2O_2$: C, 55.64; H, 3.74; N, 6.49. Found: C, 55.72; H, 3.75; N, 6.47.

4.2.21. 1-(5-Bromo-2-hydroxybenzyl)-1-(2-bromophenyl)-3-phenylurea (21)

White powder, yield 51%, mp: 160–161 °C, 1H NMR (300 MHz, $CDCl_3$): 4.64 (s, 2H); 6.07 (s, 1H); 6.71 (d, $J = 1.5$ Hz, 1H); 7.04–7.05 (m, 1H); 7.10–7.12 (m, 2H); 7.21–7.24 (m, 5H); 7.39–7.43 (m, 2H); 7.61 (d, $J = 1.5$ Hz, 1H); 10.72 (s, 1H). ESI-MS $C_{20}H_{16}Br_2N_2O_2$ $[M+H]^+$ 475.0. Anal. Calcd for $C_{20}H_{16}Br_2N_2O_2$: C, 50.45; H, 3.39; N, 5.88. Found: C, 50.34; H, 3.40; N, 5.86.

4.2.22. 1-(5-Bromo-2-hydroxybenzyl)-1-(4-bromophenyl)-3-phenylurea (22)

White powder, yield 58%, mp: 152–153 °C, ¹H NMR (300 MHz, CDCl₃): 4.64 (s, 2H); 6.09 (s, 1H); 6.75 (d, *J* = 1.4 Hz, 1H); 7.07–7.11 (m, 4H); 7.22–7.26 (m, 4H); 7.60 (d, *J* = 1.5 Hz, 1H); 7.64–7.67 (m, 2H); 10.64 (s, 1H). ESI-MS C₂₀H₁₆Br₂N₂O₂ [M+H]⁺ 475.0. Anal. Calcd for C₂₀H₁₆Br₂N₂O₂: C, 50.45; H, 3.39; N, 5.88. Found: C, 50.32; H, 3.40; N, 5.87.

4.2.23. 1-(5-Bromo-2-hydroxybenzyl)-3-phenyl-1-*p*-tolylurea (23)

White powder, yield 63%, mp: 144–145 °C, ¹H NMR (300 MHz, CDCl₃): 3.14 (s, 3H); 4.77 (s, 2H); 6.14 (s, 1H); 7.00–7.04 (m, 3H); 7.05–7.09 (m, 2H); 7.17–7.19 (m, 2H); 7.27–7.32 (m, 4H); 7.59 (d, *J* = 1.5 Hz, 1H); 10.44 (s, 1H). ESI-MS C₂₁H₁₉BrN₂O₂ [M+H]⁺ 411.0. Anal. Calcd for C₂₁H₁₉BrN₂O₂: C, 61.33; H, 4.66; N, 6.81. Found: C, 61.55; H, 4.70; N, 6.86.

4.2.24. 1-(5-Bromo-2-hydroxybenzyl)-1-(4-methoxyphenyl)-3-phenylurea (24)

White powder, yield 66%, mp: 146–147 °C, ¹H NMR (300 MHz, CDCl₃): 3.81 (s, 3H); 4.91 (s, 2H); 6.22 (s, 1H); 6.97–7.02 (m, 3H); 7.16–7.18 (m, 3H); 7.20–7.24 (m, 2H); 7.33–7.36 (m, 3H); 7.62 (d, *J* = 2.4 Hz, 1H); 10.90 (s, 1H). ESI-MS C₂₁H₁₉BrN₂O₃ [M+H]⁺ 427.1. Anal. Calcd for C₂₁H₁₉BrN₂O₃: C, 59.03; H, 4.48; N, 6.56. Found: C, 59.23; H, 4.45; N, 6.56.

4.2.25. 1-(3,5-Dibromo-2-hydroxybenzyl)-1-(2-fluorophenyl)-3-phenylurea (25)

White powder, yield 69%, mp: 150–151 °C, ¹H NMR (300 MHz, CDCl₃): 4.76 (s, 2H); 6.11 (s, 1H); 6.69 (d, *J* = 1.4 Hz, 1H); 7.05–7.09 (m, 1H); 7.15–7.18 (m, 2H); 7.26–7.33 (m, 3H); 7.47–7.52 (m, 3H); 7.60 (d, *J* = 1.4 Hz, 1H); 10.60 (s, 1H). ESI-MS C₂₀H₁₅Br₂FN₂O₂ [M+H]⁺ 493.0. Anal. Calcd for C₂₀H₁₅Br₂FN₂O₂: C, 48.61; H, 3.06; N, 5.67. Found: C, 48.48; H, 3.06; N, 5.65.

4.2.26. 1-(3,5-Dibromo-2-hydroxybenzyl)-1-(4-fluorophenyl)-3-phenylurea (26)

White powder, yield 73%, mp: 148–149 °C, ¹H NMR (300 MHz, CDCl₃): 4.78 (s, 2H); 6.12 (s, 1H); 6.70 (d, *J* = 1.4 Hz, 1H); 7.04–7.06 (m, 1H); 7.20 (d, *J* = 4.3 Hz, 2H); 7.24–7.26 (m, 3H); 7.50–7.55 (m, 3H); 7.60 (d, *J* = 1.5 Hz, 1H); 10.83 (s, 1H). ESI-MS C₂₀H₁₅Br₂FN₂O₂ [M+H]⁺ 493.0. Anal. Calcd for C₂₀H₁₅Br₂FN₂O₂: C, 48.61; H, 3.06; N, 5.67. Found: C, 48.88; H, 3.07; N, 5.70.

4.2.27. 1-(2-Chlorophenyl)-1-(3,5-dibromo-2-hydroxybenzyl)-3-phenylurea (27)

White powder, yield 58%, mp: 151–152 °C, ¹H NMR (300 MHz, CDCl₃): 4.76 (s, 2H); 6.10 (s, 1H); 6.70 (d, *J* = 1.4 Hz, 1H); 7.06–7.09 (m, 1H); 7.18–7.20 (m, 2H); 7.24–7.27 (m, 4H); 7.41–7.45 (m, 2H); 7.61 (d, *J* = 1.5 Hz, 1H); 10.75 (s, 1H). ESI-MS C₂₀H₁₅Br₂ClN₂O₂ [M+H]⁺ 508.9. Anal. Calcd for C₂₀H₁₅Br₂ClN₂O₂: C, 47.04; H, 2.96; N, 5.49. Found: C, 47.12; H, 2.98; N, 5.47.

4.2.28. 1-(4-Chlorophenyl)-1-(3,5-dibromo-2-hydroxybenzyl)-3-phenylurea (28)

White powder, yield 67%, mp: 146–147 °C, ¹H NMR (300 MHz, CDCl₃): 4.76 (s, 2H); 6.07 (s, 1H); 6.72 (d, *J* = 1.4 Hz, 1H); 7.05–7.08 (m, 1H); 7.14–7.17 (m, 2H); 7.24–7.28 (m, 5H); 7.50–7.52 (m, 1H); 7.61 (d, *J* = 1.5 Hz, 1H); 10.64 (s, 1H). ESI-MS C₂₀H₁₅Br₂ClN₂O₂ [M+H]⁺ 508.9. Anal. Calcd for C₂₀H₁₅Br₂ClN₂O₂: C, 47.04; H, 2.96; N, 5.49. Found: C, 47.17; H, 2.95; N, 5.47.

4.2.29. 1-(2-Bromophenyl)-1-(3,5-dibromo-2-hydroxybenzyl)-3-phenylurea (29)

White powder, yield 74%, mp: 161–162 °C, ¹H NMR (300 MHz, CDCl₃): 4.76 (s, 2H); 6.13 (s, 1H); 6.67 (d, *J* = 1.5 Hz, 1H); 7.06–7.09 (m, 1H); 7.12–7.14 (m, 1H); 7.26–7.28 (m, 5H); 7.37–7.44 (m, 1H); 7.45–7.47 (m, 1H); 7.61 (d, *J* = 1.5 Hz, 1H); 10.72 (s, 1H). ESI-MS C₂₀H₁₅Br₃N₂O₂ [M+H]⁺ 552.9. Anal. Calcd for C₂₀H₁₅Br₃N₂O₂: C, 43.28; H, 2.72; N, 5.05. Found: C, 43.36; H, 2.70; N, 5.06.

4.2.30. 1-(4-Bromophenyl)-1-(3,5-dibromo-2-hydroxybenzyl)-3-phenylurea (30)

White powder, yield 76%, mp: 158–159 °C, ¹H NMR (300 MHz, CDCl₃): 4.75 (s, 2H); 6.07 (s, 1H); 6.72 (d, *J* = 1.4 Hz, 1H); 7.05–7.10 (m, 3H); 7.24–7.29 (m, 4H); 7.61 (d, *J* = 1.5 Hz, 1H); 7.65–7.68 (m, 2H); 10.64 (s, 1H). ESI-MS C₂₀H₁₅Br₃N₂O₂ [M+H]⁺ 552.9. Anal. Calcd for C₂₀H₁₅Br₃N₂O₂: C, 43.28; H, 2.72; N, 5.05. Found: C, 43.43; H, 2.74; N, 5.06.

4.2.31. 1-(3,5-Dibromo-2-hydroxybenzyl)-3-phenyl-1-(*p*-tolyl)urea (31)

White powder, yield 69%, mp: 145–146 °C, ¹H NMR (300 MHz, CDCl₃): 3.30 (s, 3H); 4.78 (s, 2H); 6.07 (s, 1H); 6.71 (d, *J* = 1.5 Hz, 1H); 7.00–7.04 (m, 1H); 7.06–7.10 (m, 2H); 7.13–7.18 (m, 2H); 7.25–7.30 (m, 4H); 7.61 (d, *J* = 1.4 Hz, 1H); 10.44 (s, 1H). ESI-MS C₂₁H₁₈Br₂N₂O₂ [M+H]⁺ 489.0. Anal. Calcd for C₂₁H₁₈Br₂N₂O₂: C, 51.45; H, 3.70; N, 5.71. Found: C, 51.59; H, 3.73; N, 5.72.

4.2.32. 1-(3,5-Dibromo-2-hydroxybenzyl)-1-(4-methoxyphenyl)-3-phenylurea (32)

White powder, yield 73%, mp: 142–143 °C, ¹H NMR (300 MHz, CDCl₃): 3.77 (s, 3H); 4.80 (s, 2H); 6.17 (s, 1H); 6.98–7.02 (m, 3H); 7.14–7.17 (m, 2H); 7.21–7.26 (m, 2H); 7.35–7.38 (m, 3H); 7.63 (d, *J* = 2.4 Hz, 1H); 10.82 (s, 1H). ESI-MS C₂₁H₁₈Br₂N₂O₃ [M+H]⁺ 505.0. Anal. Calcd for C₂₁H₁₈Br₂N₂O₃: C, 49.83; H, 3.58; N, 5.53. Found: C, 49.96; H, 3.56; N, 5.54.

4.3. Antibacterial activity

The antibacterial activity of the synthesized compounds was tested against *E. coli*, *P. fluorescens*, *B. subtilis*, and *S. aureus* using MH medium (Mueller-Hinton medium: casein hydrolysate 17.5 g, soluble starch 1.5 g, beef extract 1000 mL), The MICs (minimum inhibitory concentrations) of the test compounds were determined by a colorimetric method using the dye MTT (3-(4,5-dimethylthiazol-2-yl)-2,5-diphenyl tetrazolium bromide). A stock solution of the synthesized compound (100 µg/mL) in DMSO was prepared and graded quantities of the test compounds were incorporated in specified quantity of sterilized liquid MH medium. A specified quantity of the medium containing the compound was poured into microtitration plates. Suspension of the microorganism was prepared to contain approximately 10⁵ cfu/mL and applied to microtitration plates with serially diluted compounds in DMSO to be tested and incubated at 37 °C for 24 h. After the MICs were visually determined on each of the microtitration plates, 50 µL of PBS (phosphate buffered saline 0.01 mol/L, pH 7.4: Na₂HPO₄·12H₂O 2.9 g, KH₂PO₄ 0.2 g, NaCl 8.0 g, KCl 0.2 g, distilled water 1000 mL) containing 2 mg of MTT/mL was added to each well. Incubation was continued at room temperature for 4–5 h. The content of each well was removed, and 100 µL of isopropanol containing 5% 1 mol/L HCl was added to extract the dye. After 12 h of incubation at room temperature, the optical density (OD) was measured with a microplate reader at 550 nm.

4.4. *E. coli* FabH purification and activity assay

Native *E. coli* FabH protein was overexpressed in *E. coli* DH10B cells using the pET30 vector and purified to homogeneity in three chromatographic steps (Q-Sepharose, MonoQ, and hydroxyapatite) at 4 °C. The selenomethionine-substituted protein was expressed in *E. coli* BL21(DE3) cells and purified in a similar way. Harvested cells containing FabH were lysed by sonication in 20 mM Tris, pH 7.6, 5 mM imidazole, 0.5 M NaCl and centrifuged at 20,000 rpm for 30 min. The supernatant was applied to a Ni-NTA agarose column, washed, and eluted using a 5–500 mM imidazole gradient over 20 column volumes. Eluted protein was dialyzed against 20 mM Tris, pH 7.6, 1 mM DTT, and 100 mM NaCl. Purified FabHs were concentrated up to 2 mg/mL and stored at –80 °C in 20 mM Tris, pH 7.6, 100 mM NaCl, 1 mM DTT, and 20% glycerol for enzymatic assay.

In a final 20 μ L reaction, 20 mM Na₂HPO₄, pH 7.0, 0.5 mM DTT, 0.25 mM MgCl₂, and 2.5 μ M holo-ACP were mixed with 1 nM FabH, and H₂O was added to 15 μ L. After 1 min incubation, a 2 μ L mixture of 25 μ M acetyl-CoA, 0.5 mM NADH, and 0.5 mM NADPH was added for FabH reaction for 25 min. The reaction was stopped by adding 20 μ L of ice-cold 50% TCA, incubating for 5 min on ice, and centrifuging to pellet the protein. The pellet was washed with 10% ice-cold TCA and resuspended with 5 μ L of 0.5 M NaOH. The incorporation of the ³H signal in the final product was read by liquid scintillation. When determining the inhibition constant (IC₅₀), inhibitors were added from a concentrated DMSO stock such that the final concentration of DMSO did not exceed 2%.^{29,30}

4.5. Docking simulations

Molecular docking of synthetic compounds into the three-dimensional X-ray structure of *E. coli* FabH (PDB code: 1HNJ) was carried out using the AUTODOCK software package (version 4.0) as implemented through the graphical user interface AutoDockTools (ADT 1.4.6).³¹

Acknowledgment

This work was supported by Jiangsu National Science Foundation (No. BK2009239) and the Fundamental Research Fund for the Central Universities (No. 1092020804).

References and notes

1. Leeb, M. *Nature* **2004**, 431, 892.
2. Khalafi-Nezhad, A.; Rad, M. N. S.; Mohabatkar, H.; Asrari, Z.; Hemmateenejad, B. *Bioorg. Med. Chem.* **2005**, 13, 1931.
3. Lee, J.-Y.; Jeong, K.-W.; Lee, J.-U.; Kang, D.-I.; Kim, Y. *Bioorg. Med. Chem.* **2009**, 17, 1506.
4. Ali, A.; Seung, J. C. *Bioorg. Med. Chem.* **2006**, 14, 1474.
5. Puupponen-Pimiä, R.; Nohynek, L.; Meier, C.; Kähkönen, M.; Heinonen, A. H. J. *Appl. Microbiol.* **2001**, 90, 494.
6. Herbert, P. S. *FEMS Microbiol. Lett.* **2001**, 202, 1.
7. Rock, C. O.; Jackowski, S. *Res. Commun.* **2002**, 292, 1155.
8. Roberts, C. W.; McLeod, R.; Rice, D. W. *Mol. Biochem. Parasit.* **2003**, 126, 129.
9. McMurray, L. M.; Oethinger, M.; Levy, S. B. *Nature* **1998**, 394, 531.
10. Perozzo, R.; Kuo, M.; Sidh, A. S. *Biol. Chem.* **2002**, 277, 151.
11. Sharada, S.; Jacque, Z.; Alasdair, F. Bell.; Lizbeth, H.; Peter, J. T. *Biochemistry* **2003**, 42, 4406.
12. Sharada, S.; Todd, J. S.; Francis, J.; Polina, N.; Guanglei, C.; Carlos, S.; Peter, J. J. *Med. Chem.* **2004**, 47, 509.
13. Heath, R. J.; White, S. W.; Rock, C. O. *Appl. Microbiol. Biot.* **2002**, 58, 695.
14. Ozaki, S. *Chem. Rev.* **1972**, 72, 457.
15. Hwang, K. J.; Park, K. H.; Lee, C. O.; Kim, B. T. *Arch. Pharm. Res.* **2002**, 25, 781.
16. Shimshoni, J. A.; Bialer, M.; Wlodarczyk, B.; Finnell, R. H.; Yagen, B. *J. Med. Chem.* **2007**, 50, 6419.
17. Knight, R. L.; Meier, D.; Oliver, K.; Meissner, J. W. G.; Owen, D. A.; Thomas, E. J.; Tremayne, N.; Williams, S. C. *Bioorg. Med. Chem. Lett.* **2008**, 18, 147.
18. Kumar, M.; Hosur, M. V. *Eur. J. Biochem.* **2003**, 270, 1231.
19. Dai, Y.; Hartandi, K.; Ji, Z.; Ahmed, A. A.; Albert, D. H.; Bauch, J. L.; Bouska, J. J.; Bousquet, P. F.; Cunha, G. A.; Glaser, K. B.; Harris, C. M.; Hickman, D.; Guo, J.; Li, J.; Marcotte, P. A.; Marsh, K. C.; Moskey, M. D.; Martin, R. L.; Olson, A. M.; Osterling, D. J.; Pease, L. J.; Soni, N. B.; Stewart, K. D.; Stoll, V. S.; Tapang, P.; Reuter, D. R.; Davidsen, S. K.; Michaelides, M. R. *J. Med. Chem.* **2007**, 50, 1584.
20. Song, E. Y.; Kaur, N.; Park, M. Y.; Jin, Y.; Lee, K.; Kim, G.; Lee, K. Y.; Yang, J. S.; Shin, J. H.; Nam, K. Y.; No, K. T.; Han, G. *Eur. J. Med. Chem.* **2008**, 43, 1519.
21. Morré, D. J.; Wu, L.-Y.; Morré, D. M. *Biochim. Biophys. Acta* **1995**, 1240, 11.
22. De, S. B.; Saftig, P.; Craessaerts, K.; Vanderstichele, H.; Guhde, G.; Annaert, W.; Von, F. K.; Van, L. F. *Nature* **1998**, 391, 387.
23. Ohnuma, S.; Muraoka, M.; Ioriya, K.; Ohashi, N. *Bioorg. Med. Chem. Lett.* **2004**, 14, 1309.
24. Li, H. Q.; Yan, T.; Lv, P. C.; Zhu, H. L. *Anti-Cancer Agents Med. Chem.* **2009**, 9, 471.
25. Li, H. Q.; Zhu, T. T.; Yan, T.; Luo, Y.; Zhu, H. L. *Eur. J. Med. Chem.* **2009**, 44, 453.
26. Esteves-Souza, A.; Echevarria, A.; Sant Anna, C. M. R.; Nascimento, M. G. *Quim. Nova* **2004**, 27, 72.
27. He, X.; Anne, M. R.; Umesh, R. D.; Glen, E. K.; Kevin, A. R. *Antimicrob. Agents Chemother.* **2004**, 48, 3093.
28. Qiu, X.; Janson, C. A.; Smith, W. W.; Head, M.; Lonsdale, J.; Konstantinidis, A. K. *J. Mol. Biol.* **2001**, 307, 341.
29. Cheng, K.; Zheng, Q. Z.; Qian, Y.; Shi, L.; Zhao, J.; Zhu, H. L. *Bioorg. Med. Chem.* **2009**, 17, 7861.
30. Shi, L.; Fang, R. Q.; Zhu, Z.; Wei, Yang, Y.; Cheng, K.; Zhong, W. Q.; Zhu, H. L. *Eur. J. Med. Chem.* **2010**, 45, 4358.
31. Huey, R.; Morris, G. M.; Olson, A. J.; Goodsell, D. S. *J. Comput. Chem.* **2007**, 28, 1145.